B cell c-Maf signaling promotes tumor progression in animal models of pancreatic cancer and melanoma

Qian Zhong,[1] Hongying Hao,[2] Shu Li,[1] Yongling Ning,[1] Hong Li,[1] Xiaoling Hu,[1] Kelly M McMasters,[2] Jun Yan ![ORCID] ,[1,2] Chuanlin Ding ![ORCID] [1,2]

¹UofL Health Brown Cancer Center, University of Louisville School of Medicine, Louisville, Kentucky, USA
²The Hiram C. Polk, Jr., MD Department of Surgery, University of Louisville, Louisville, Kentucky, USA

Correspondence to
Dr Chuanlin Ding;
chuanlin.ding@louisville.edu

ABSTRACT

Background The role of B cells in antitumor immunity remains controversial, with studies suggesting the protumor and antitumor activity. This controversy may be due to the heterogeneity in B cell populations, as the balance among the subtypes may impact tumor progression. The immunosuppressive regulatory B cells (Breg) release interleukin 10 (IL-10) but only represent a minor population. Additionally, tumor-specific antibodies (Abs) also exhibit antitumor and protumor functions dependent on the Ab isotype. Transcription factor c-Maf has been suggested to contribute to the regulation of IL-10 in Breg, but the role of B cell c-Maf signaling in antitumor immunity and regulating Ab responses remains unknown.

Methods Conditional B cell c-Maf knockout (KO) and control mice were used to establish a KPC pancreatic cancer model and B16.F10 melanoma model. Tumor progression was evaluated. B cell and T cell phenotypes were determined by flow cytometry, mass cytometry, and cytokine/chemokine profiling. Differentially expressed genes in B cells were examined by using RNA sequencing (RNA-seq). Peripheral blood samples were collected from healthy donors and patients with melanoma for B cell phenotyping.

Results Compared with B cells from the spleen and lymph nodes (LN), B cells in the pancreas exhibited significantly less follicular phenotype and higher IL-10 production in naïve mice. c-Maf deficiency resulted in a significant reduction of CD9⁺ IL-10-producing Breg in the pancreas. Pancreatic ductal adenocarcinoma (PDAC) progression resulted in the accumulation of circulating B cells with the follicular phenotype and less IL-10 production in the pancreas. Notably, B cell c-Maf deficiency delayed PDAC tumor progression and resulted in proinflammatory B cells. Further, tumor volume reduction and increased effective T cells in the tumor-draining LN were observed in B cell c-Maf KO mice in the B16.F10 melanoma model. RNA-seq analysis of isolated B cells revealed that B cell c-Maf signaling modulates immunoglobulin-associated genes and tumor-specific Ab production. We furthermore demonstrated c-Maf-positive B cell subsets and an increase of IL-10-producing B cells after incubation with IL-4 and CD40L in the peripheral blood of patients with melanoma.

Conclusion Our study highlights that B cell c-Maf signaling drives tumor progression through the modulation of Breg, inflammatory responses, and tumor-specific Ab responses.

WHAT IS ALREADY KNOWN ON THIS TOPIC

⇒ The net effect of B cells on tumor immunity depends on the balance of various B cell subtypes. c-Maf has been suggested to contribute to the regulation of interleukin 10 in regulatory B cells, but the role of B cell c-Maf signaling in antitumor immunity remains unknown.

WHAT THIS STUDY ADDS

⇒ This study shown that B cell c-Maf signaling drives tumor progression in pancreatic cancer and melanoma. We defined different antitumor mechanisms of B cell c-Maf deficiency in two tumor models. Specifically, c-Maf signaling modulates the proinflammatory phenotype of B cells in the KPC tumor-bearing pancreas and tumor-specific antibody responses in tumor draining lymph nodes of melanoma.

HOW THIS STUDY MIGHT AFFECT RESEARCH, PRACTICE OR POLICY

⇒ These studies indicate that inhibition of c-Maf signaling is a novel and promising approach for immunotherapy in pancreatic cancer and melanoma.

BACKGROUND

B cells are known to regulate immunity by producing specific antibodies (Abs), secreting cytokines, serving as antigen-presenting cells (APCs) to promote T cell responses, and forming tumor-associated tertiary lymphoid structures. Previous studies have demonstrated that B cells are significantly expanded in the pancreas and contribute to the development of pancreatic ductal adenocarcinoma (PDAC).[1 2] Further, tumor progression results in significant B cell expansion and activation in tumor-draining lymph nodes (TDLN),[3 4] which can simultaneously modulate antitumor immunity and metastatic potential.[5 6]

Although B cells are generally thought to augment immune responses and antitumor immunity,[7–11] B cells also suppress immune responses in a variety of mouse models of

cancer.[12–15] This controversy may be due to the fact that B cells have multiple subsets depending on their stage of development and function. Regulatory B cells (Breg) exhibit immunosuppressive functions by secreting cytokines (interleukin (IL)-10, IL-35, and TGF-β) and inducing regulatory T cell differentiation,[2 15–18] but the immunosuppressive Breg represent a minor cell population of B cells. The protumor effect of Breg might be overcome by the presence of other subsets of B cells. Therefore, the net effect of B cells on tumor immunity depends on the balance of various B cell subtypes.[19 20] In addition, the transcriptional regulation of Breg in the tumor microenvironment and TDLN remains poorly understood. We postulate that targeting Breg could improve antitumor responses by reversing their protumor effects.

It has been shown that transcription factor c-Maf plays an essential role in regulating of T cells and myeloid cells.[16] Our previous studies have demonstrated that c-Maf is overexpressed in tumor-associated macrophages and γδT17 cells and is associated with their protumor effect.[17 18] Although c-Maf has been suggested to contribute to Breg differentiation,[21–23] the roles of B cell c-Maf signaling in antitumor immunity remain unknown. In this study, we demonstrate that specific knockout (KO) of c-Maf in B cells inhibits tumor progression in animal models of PDAC and melanoma, which is associated with an increase of effector T cells. In addition to the regulation of IL-10 production, our study also suggests that c-Maf can regulate B cell inflammatory responses and tumor-specific Ab responses in mouse models of PDAC and melanoma, respectively.

RESULTS
c-Maf regulates pancreas B1 cells and B cell IL-10 expression
Whole B cells express low levels of transcription factor c-Maf.[24] We performed flow cytometry analysis and found that c-Maf expression is relatively high in CD9^{+} B cells and these cells produce IL-10.[25] Western blotting verified that c-Maf is remarkably downregulated in the CD9^{+} B cells of conditional B cell c-Maf KO mice (online supplemental figure 1A). We further used IL-10[gfp] reporter mice and found that c-Maf is expressed in IL-10^{+} B cells at relatively higher levels (online supplemental figure 1B,C).

Prior studies highlight that tumor location contributes to the discrepancy of B cell function in tumors.[8 26 27] Naïve peripheral B cells can be generally divided into three subsets: Follicular B cells, marginal zone (MZ) B cells and B1 cells. The comparison of B cell subsets among tissues and the impact of B cell c-Maf signaling have not been reported. To better understand the role of B cell in tumor immunity in different tissues, we started by examining the distribution of B cell subpopulations in the spleen, lymph nodes (LN), and pancreas from naive control and B cell c-Maf KO mice using flow cytometry, and the gating strategy was shown in online supplemental figure 2. As shown in figure 1A,B cells in the pancreas exhibited significantly less follicular phenotype compared with B

cells from the spleen and LN. c-Maf deficiency did not alter the composition of follicular B cells and MZ B cells. Naïve B cells express B cell receptor (BCR), including immunoglobulin (Ig)M and IgD isotype. Compared with the B cells in the spleen and LN, the pancreas had more IgD[low]IgM^{+} B cells and fewer IgD[+]IgM^{low} B cells. c-Maf deficiency did not impact the composition of IgD[+]IgM^{low} B cells and IgD[low]IgM^{+} B cells in these tissues (figure 1B).

B1 cells are a small but unique subpopulation of B cells that can constitutively produce IL-10.[28] There are two subsets of B1 cells: CD5^{+} B1a and CD5^{−} B1b. Compared with the spleen and LN, the pancreas was infiltrated with more B1a and B1b cells. c-Maf deficiency decreased pancreas B1a and B1b cells as well as spleen B1a cells. No significant changes of B1a and B1b cells were observed in LN between control and B cell c-Maf KO mice (figure 1C). We further examined IL-10 production in spleen, LN, and pancreas B cells from control and B cell c-Maf KO mice. Notably, we observed a significantly greater population of CD9^{+}IL-10^{+} B cells in the pancreas, which was correlated with an increase of B1 cells in the pancreas. c-Maf deficiency significantly reduced the proportion of CD9^{+} IL-10-producing B cells in the pancreas (figure 1D). Together, these data suggest that B cells in the pancreas exhibit a distinct phenotype. B cell c-Maf signal modulates B cell IL-10 expression in the pancreas under steady state conditions.

Tumor progression induces complexity of B cell phenotype in pancreas
Previous studies have shown that B cells exhibit immunosuppressive roles in the KPC mouse model of pancreatic cancer, especially IL-35-producing B cells.[14 15 20] However, it was also reported that B cells upregulate several proinflammatory and immunostimulatory genes on tumor progression.[29] Therefore, the phenotype and function of B cells as a whole population in the KPC tumor model are still not well understood. Subsets of infiltrating B cells in the pancreas during tumor progression have not been thoroughly investigated. To understand the changes of B cell phenotype and function during tumor progression, we evaluated the distribution of B cells and their subpopulations in the pancreas from tumor-free and KPC tumor-bearing mice by flow cytometry. KPC tumor development induced a significant infiltration of CD19^{+} B cells in the pancreas, including the increased percentage of CD19^{+} B cells within CD45^{+} leukocytes (figure 2A) and an increased absolute number of B cells (figure 2B). The expanded B cells mainly exhibited follicular B cell phenotype (CD23^{+}CD21^{low}) (figure 2C). Accordingly, IgD^{+}IgM^{low} B cells were increased whereas IgD^{low}IgM^{+} B cells were decreased in the tumor-bearing pancreas (figure 2D).

To examine B cell phenotypic changes on tumor development, B cells were isolated from tumor-free and KPC tumor-bearing pancreas and stimulated with lipopolysaccharides (LPS) for 3 days. As shown in figure 2E, the tumor-infiltrating B cells proliferated extensively on LPS
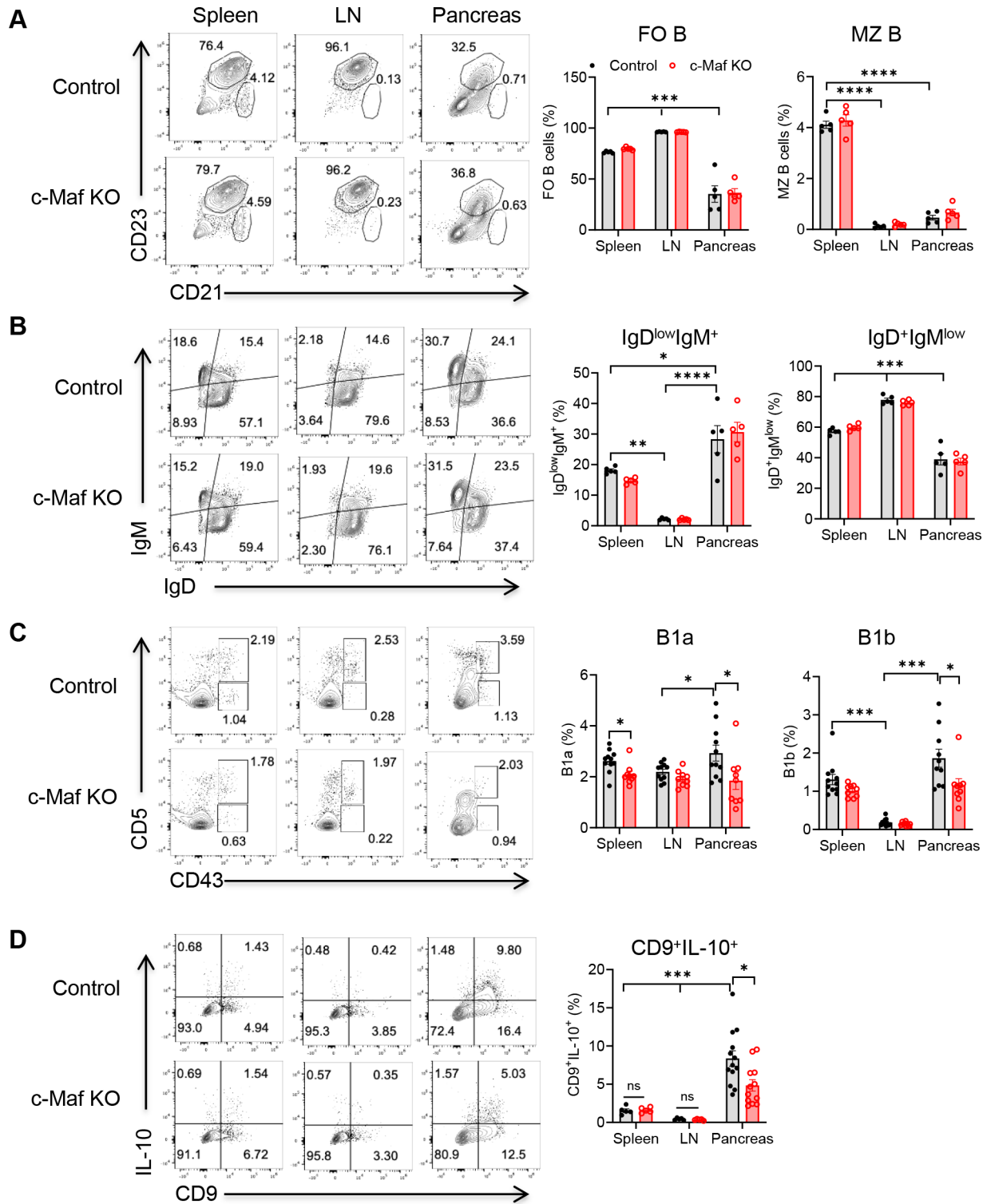
Figure 1 B cell subsets and B cell IL-10 expression in spleen, lymph node, and pancreas of naïve control and c-Maf KO mice. (A) Follicular B cells (FO, CD21^{low}CD23$^+$) and marginal zone B cells (MZ, CD21$^+$CD23$^-$) within CD19$^+$ B cells. (B) IgD and IgM expression by B cells. (C) B1a (CD43$^+$CD5$^+$) and B1b (CD43$^+$CD5$^-$) within CD19$^+$IgM$^+$ B cells. (D) IL-10 production by CD9$^+$ B cells after 4–6 hour of PMA/Ionomycin/LPS stimulation. Representative plots and summarized results are shown. Each point represents an individual mouse (n=5–13). *p<0.05; **p<0.01; ***p<0.001; ****p<0.0001. FO, follicular B cells; Ig, immunoglobulin; IL-10, interleukin 10; KO, knockout; LN, lymph node; LPS, lipopolysaccharides; MZ, marginal zone B cells; PMA, phorbol 12-myristate 13-acetate.

stimulation. Further, isolated B cells were stimulated them with phorbol 12-myristate 13-acetate (PMA)/Ionomycin/LPS for 24 hours and culture supernatants from stimulated

B cells were collected for cytokine and chemokine assay. The array analysis revealed that tumor-infiltrating B cells secreted a vast array of proteins on ex vivo stimulation.
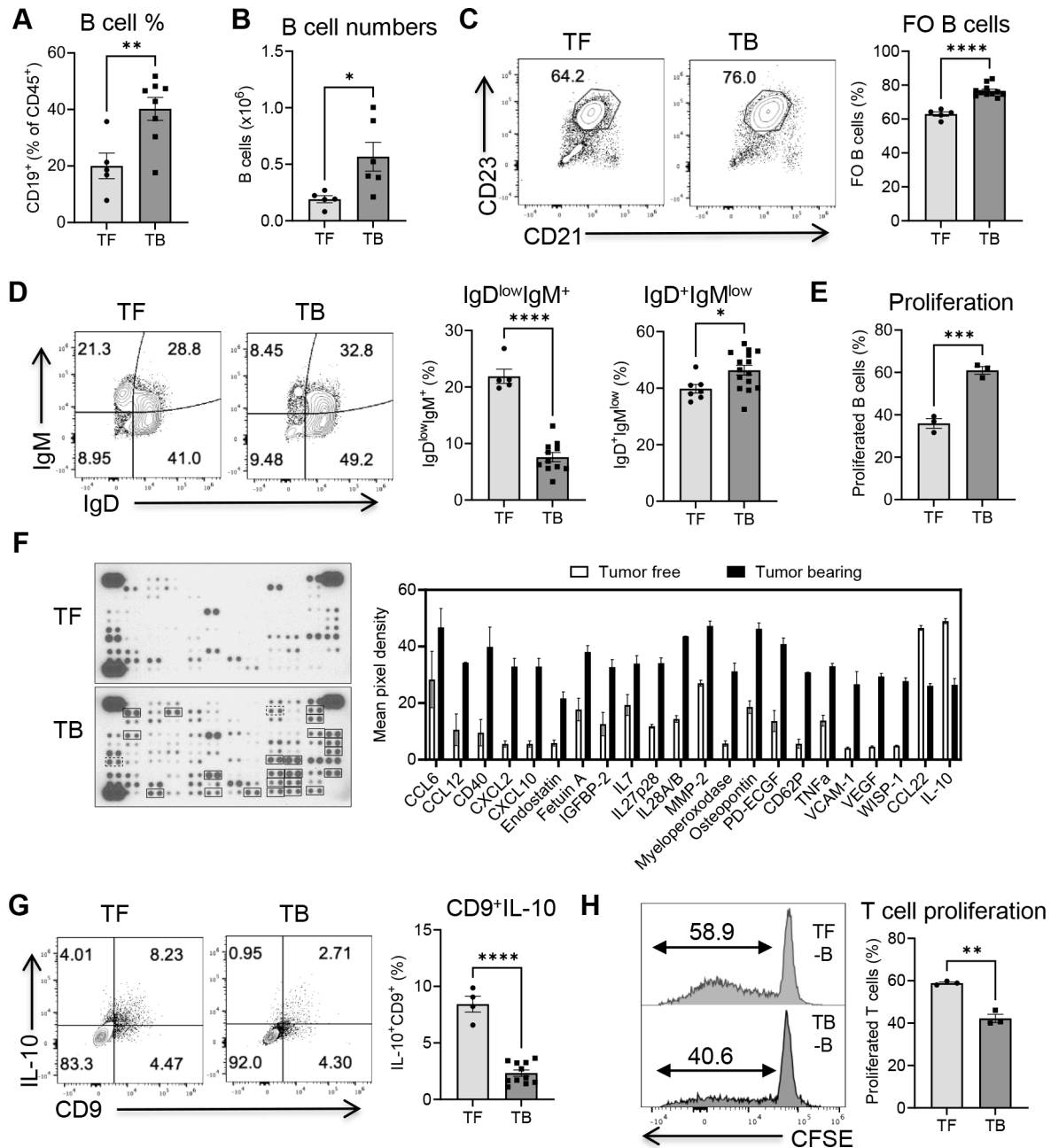
Figure 2 Tumor progression induces a complex B cell phenotype in pancreas. 8–10 weeks old B6 wild-type mice were implanted orthotopically with KPC pancreatic cancer cells. (A) Percentages of CD19^{+} B cells within CD45^{+} leukocytes in tumor-free (TF) and tumor-bearing (TB) mice. (B) Absolute cell numbers of B cells in the pancreas of TF and TB mice. (C) Percentages of follicular B cells within CD19^{+} B cells. (D) IgD and IgM expression by B cells. Each point represents an individual mouse (n=5–11). (E) B cell proliferation after 3 days culture in the presence of LPS (1 μg/mL). (F) Cytokine/chemokine array of culture supernatants of isolated B cells. The mean pixel intensity of differentially expressed molecules was measured using ImageJ software. (G) IL-10 production by B cells after ex vivo stimulation with PMA/Ionomycin/LPS. (H) T cell proliferation of OT-II CD4^{+} T cells after co-culture with isolated B cells in the presence of OVA for 4 days. *p<0.05; **p<0.01; ***p<0.001; ****p<0.0001. CFSE, carboxyfluorescein succinimidyl ester; FO, follicular B cells; Ig, immunoglobulin; IL-10, interleukin 10; LPS, lipopolysaccharides; OVA, ovalbumin; PMA, phorbol 12-myristate 13-acetate.

Several cytokines and chemokines, such as CCL6, CCL12, CXCL2, CXCL10, IL7, IL27, IL28, and TNF-α, were highly expressed in tumor-infiltrating B cells. Interestingly, downregulation of IL-10 and CCL22 was observed in the culture supernatants of tumor-infiltrating B cells (figure 2F). In agreement, the percentage of CD9^{+}IL-10^{+} B cells was also decreased in the tumor-bearing pancreas

(figure 2G). This could be explained by the fact that more follicular B cells are circuited and infiltrated into the pancreas in response to tumor progression.

To determine the net impact of B cells on T cell activation, total B cells (CD45^{+}CD19^{+} B cells) were sorted from the pancreas of tumor-free and KPC tumor-bearing mice and co-cultured with purified CD3^{+}CD4^{+} OT-II T cells.

As expected, B cells from tumor-bearing mice exhibited decreased antigen presentation function for T cell activation (figure 2H). Together, these data illustrate that tumor progression induces a complex B cell phenotype in the pancreas. B cells as a whole population exhibit a proinflammatory phenotype and decreased antigen-presenting capability.

B cell c-Maf deficiency delays tumor progression in mouse PDAC model

Given that c-Maf regulates B cell IL-10 expression in the pancreas, we investigated the roles of B cell intrinsic c-Maf signaling in regulating antitumor immunity in the mouse PDAC model. 1×10^5 KPC-GFP cells were mixed with Matrigel at a 1:1 ratio, and a 50 μl mixture was orthotopically implanted into the tail of the pancreas of 8–10 weeks old B cell c-Maf KO and control mice. Pancreas were collected at day 18–21 post-tumor cell implantation. As shown in figure 3A, both pancreas weight and the amount of GFP$^+$ KPC tumor cells showed a decrease in B cell c-Maf KO mice. IL-10$^+$ B cells were also decreased in c-Maf KO mice, although overall B cell percentages were not changed (figure 3A). Accordingly, effective T cells (CD4$^+$IFN-γ$^+$, CD8$^+$IFN-γ$^+$) were significantly increased in the tumor-bearing pancreas of B cell c-Maf KO mice (figure 3B). To determine whether B cell c-Maf deficiency directly impacts T cell activation, total CD19$^+$ B cells were sorted from KPC tumor-bearing pancreas of control and c-Maf KO mice and co-cultured with FACS-isolated CD3$^+$CD4$^+$ OT-II T cells in the presence of antigen ovalbumin (OVA). T cells proliferated at a similar rate when co-cultured with control or c-Maf-deficient B cells (figure 3C), suggesting that B cell c-Maf deficiency has no direct effect on T cell activation when using the whole B cell population as APCs.

To investigate how c-Maf deficiency in B cells affects tumor progression, we analyzed gene profiles of B cells using RNA sequencing (RNA-seq). Altogether, 1,266 genes were differentially expressed between tumor-educated control and c-Maf-deficient B cells (figure 3D). Interestingly, several chemokines, including CCL3, CCL6, CCL9, CCL7, CCL17, CXCL12, CXCL10, and CXCL16, were upregulated in c-Maf-deficient B cells (figure 3E). IL-10 expression showed a decreased trend in c-Maf KO B cells compared with control B cells. This decrease was not significant because of the variation. Next, functional annotation of genes in tumor-educated c-Maf deficient B cells compared with control B cells was performed. c-Maf deficient B cells were uniquely enriched in gene sets associated with inflammatory response and chemotaxis (figure 3F). We further isolated B cells and stimulated with PMA/Ionomycin/LPS for 24 hours and collected culture supernatants for cytokine and chemokine analysis. Compared with the B cells from tumor-bearing control mice, B cell c-Maf deficiency resulted in an increase of CCL22, Cysatin C, CXCL5, CXCL10, IL-11, and TNF-α (figure 3G). These molecules have been shown to have proinflammatory effects in previous studies.[30–32] The

data are consistent with previous findings that B cells can sustain inflammation and predict response to immune checkpoint blockade (ICB),[33] and that proinflammatory chemokines can boost natural killer (NK) and T cell recruitment leading to immunological tumor control.[34] Similar levels of IL-10 in the B cell culture supernatants of KPC tumor-bearing control and KO mice were observed (figure 3G, spot G1, 2). This inconsistent data might be due to the limited number of mice used in different experiments. It may be also because total B cells were used in the ex vivo culture. Only a small fraction of CD9$^+$ B cells was present. Together, our data suggest that B cell c-Maf signaling exhibits a protumor effect in the KPC tumor model via regulation of a proinflammatory phenotype in B cells.

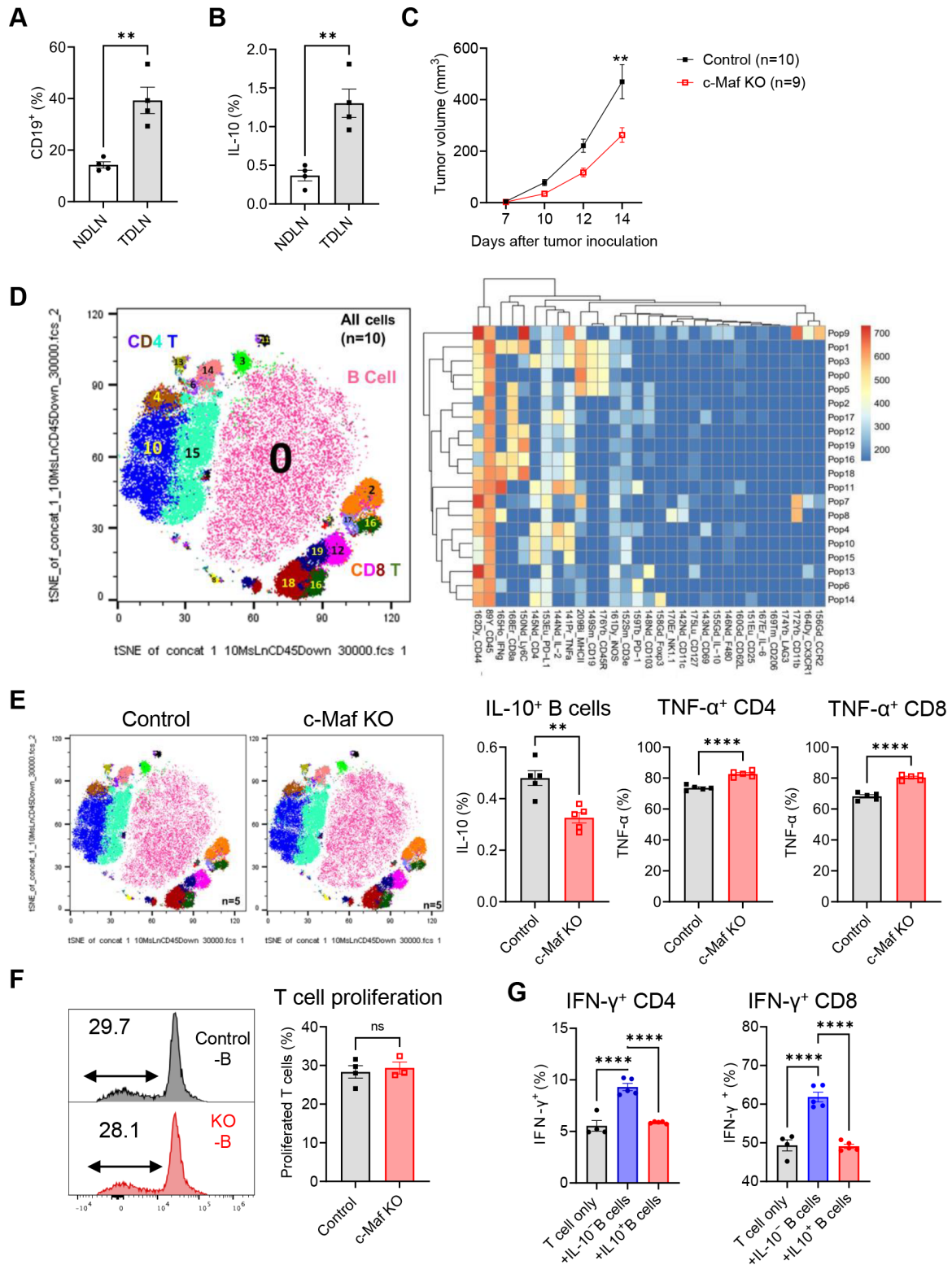## B cell c-Maf deficiency reduces B16.F10 melanoma tumor progression

For many solid tumors, LN remodeling contributes to both metastatic potential and immune surveillance.[5] Previous studies have shown that B cells are significantly expanded in the TDLN and promote breast cancer metastasis.[3] It was also reported that there is an accumulation of regulatory transitional 2-MZ precursor B cells in TDLN of B16.F10 melanoma tumor-bearing mice.[4] Our data confirmed the expansion of B cells in the TDLN of the B16.F10 tumor (figure 4A). Importantly, IL-10-producing B cells were also increased in the TDLN of B16.F10 tumor (figure 4B). To determine whether B cell c-Maf signaling plays roles in melanoma, control and B cell c-Maf KO mice were injected subcutaneously with B16.F10 melanoma cells in the flank. As shown in figure 4C, B16.F10 tumor progression in B cell c-Maf KO mice was significantly reduced compared with control mice.

Next, we used mass cytometry (CyTOF) to determine the effect of B cell c-Maf deficiency on immune cell profiling within TDLN after ex vivo restimulation with PMA/Ionomycin plus LPS in the presence of brefeldin A for 4–6 hours. FlowSOM analysis identified a total of 20 immune cell subtypes, including B cells (population 0, 1, 3, and 5), CD4 T cells (populations 4, 10, 15, 6, 14, and 11), and CD8 T cells (populations 2,12, 16, 17, 18, and 19) (figure 4D). Although B c-Maf deficiency did not impact the composition of these major cell subsets, IL-10 production was reduced in c-Maf-deficient B cells, which was associated with an increase of effective TNF-α$^+$ CD4$^+$ and CD8$^+$ T cells (figure 4E).

To evaluate whether B cell c-Maf deficiency has a direct effect on T cell activation, total CD19$^+$ B cells were sorted from TDLN of control and c-Maf KO B16.F10 tumor-bearing mice and co-cultured with FACS-isolated CD3$^+$CD4$^+$ OT-II T cells in the presence of antigen OVA. T cells proliferated at a similar rate when co-cultured with control or c-Maf-deficient B cells (figure 4F), suggesting that B cell c-Maf deficiency has no direct effect on T cell activation when using the whole B cell population as APCs. This could be explained by the fact that immunosuppressive B cells represent a relatively minor
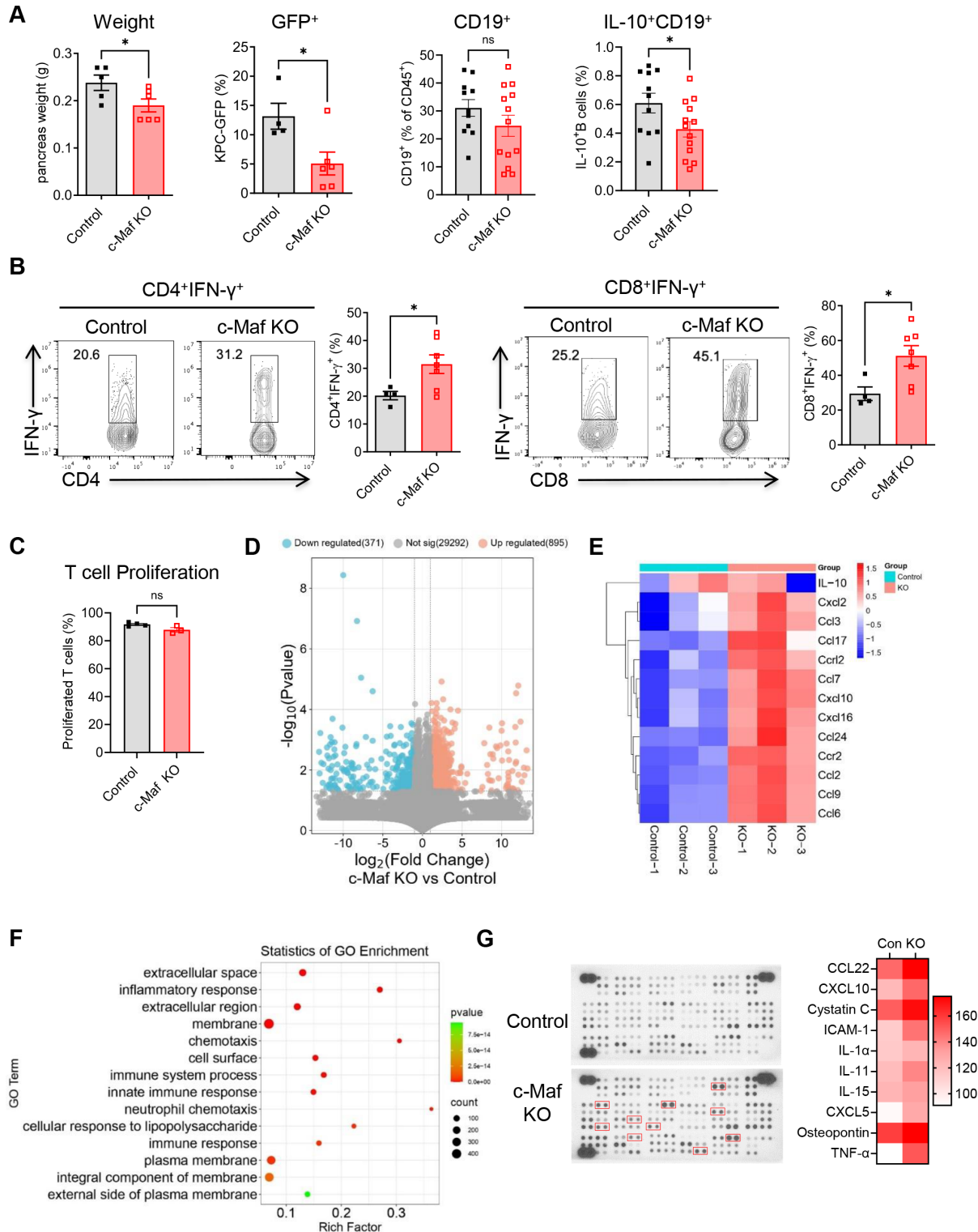
Figure 3 B cell c-Maf deficiency delays tumor progression in the PDAC mouse model. (A) Pancreas weight, percentages of GFP$^+$ tumor cells within CD45$^-$ pancreas cells, CD19$^+$ B cells within CD45$^+$ leukocytes, and IL-10-producing B cells of KPC tumor-bearing control and c-Maf KO mice. Each point represents an individual mouse (n=5–13). (B) IFN-γ production by CD4$^+$ and CD8$^+$ T cells after ex vivo restimulation with PMA/Ionomycin. (C) T cell proliferation of OT-II CD4$^+$ T cells after co-culture with FACS-isolated control and c-Maf KO B cells. (D) Volcano plot showing fold change (FC) and p value for the comparison of B cells from control versus c-Maf KO mice based on RNA sequencing data (n=3). (E) Heatmap showing the clustering of chemokines in two groups based on log-relative abundances. (F) GO enrichment analysis of genes defining the 14 most significant terms. (G) Cytokine/chemokine array of culture supernatants of isolated B cells (pooled samples from three control and KO mice). The mean pixel intensity of differentially expressed molecules was measured using ImageJ software. *p<0.05; ns, not significant. FACS, fluorescence-activated cell sorting; GO, Gene Ontology; IL-10, interleukin 10; KO, knockout; PDAC, pancreatic ductal adenocarcinoma; PMA, phorbol 12-myristate 13-acetate.

Figure 4 B cell c-Maf deficiency inhibits B16.F10 melanoma tumor progression. (A) Percentages of CD19⁺ B cells within CD45⁺ leukocytes in TDLN of tumor-bearing mice. (B) Percentages of IL-10-producing B cells in TDLN of tumor-bearing mice compared with that in NDLN. (C) Tumor progression in control and c-Maf KO mice (n=9–10). (D) viSNE analysis of CyTOF immunophenotyping of TDLN from tumor-bearing control and c-Maf KO mice, all samples combined (n=10, left). FlowSOM clustering into 20 final immune cell types showing as a normalized expression heatmap (right). (E) viSNE analysis of CyTOF immunophenotyping in TDLN of control and c-Maf KO mice (n=5). Percentages of IL-10-producing B cells, TNF-α⁺ CD4⁺ and CD8⁺ T cells were summarized. (F) T cell proliferation of OT-II CD4⁺ T cells after co-culture with isolated B cells (G) IFN-γ production by anti-CD3 mAb-activated CD4⁺ and CD8⁺ T cells after co-culture with IL-10⁻ and IL-10⁺ B cells. **p<0.01; ****p<0.0001; ns, not significant. CyTOF, mass cytometry; IL-10, interleukin 10; KO, knockout; NDLN, non-draining lymph nodes; TDLN, tumor-draining lymph nodes.

cell population. To confirm this possibility, we cultured B cells from IL-10^gfp reporter mice using NIH3T3/CD40LB feeder cells and cytokines (IL-4, IL-21).[35] IL-10-producing B cells (eGFP^+) and IL-10-negative B cells (eGFP^-) were sorted and co-cultured with anti-CD3 activated T cells (figure 4G and online supplemental figure 3), IL-10-negative B cells enhanced IFN-γ production by CD4 and CD8 T cells, whereas IL-10-producing B cells exhibited immunosuppressive effects compared with IL-10-negative B cells. Together, these data suggest that B cell c-Maf signaling exhibits protumor effects in melanoma, which might not be through direct B cell/T cell interaction.

c-Maf regulates Ig-related genes in B cells and tumor-specific Ab production

To understand how B cell c-Maf signaling regulates antitumor immunity in melanoma, we purified B cells from LN of naïve mice and TDLN of B16.F10 tumor-bearing control and B cell c-Maf KO mice and performed RNA-seq. A comparison of differentially expressed genes among different groups was illustrated in a Venn diagram (figure 5A). Several genes related to Ig, such as *Jchain, Ighg2b, Ighv1-37, Igkv3-12, Igkv8-21, Iglv1, Ighg3*, were significantly upregulated in the tumor-bearing B cells compared with the naïve B cells (figure 5B,F). B cell c-Maf deficiency resulted in a significant decrease of these genes in tumor-bearing animals (figure 5C,F). Gene ontology enrichment analysis showed that factors involved in circulating Ig complex, Ig production, and external side of plasma membrane were enriched in the tumor-bearing B cells compared with naïve B cells (figure 5D). These factors were regulated by c-Maf because these pathways were significantly enriched in the c-Maf deficient tumor-bearing B cells compared with control B cells (figure 5E), suggesting the important roles of c-Maf in regulating Ab responses.

It is known that Ab isotype can influence antitumor immunity.[36 37] Next, we collected sera from tumor-bearing mice at day 14 post-tumor cell inoculation and measured B16.F10 tumor-specific Abs and their isotype by incubating sera with tumor cells followed by flow cytometry. As shown in figure 5G, antitumor IgG1, IgG2a, IgG2b Abs were decreased in the B cell c-Maf KO tumor-bearing mice, suggesting a modulatory effect of B cell c-Maf signaling on in vivo Ab responses.

B cell profiling in the peripheral blood of patients with melanoma

To explore the clinical significance of the study, peripheral blood mononuclear cells (PBMCs) of healthy donors (HD) were stimulated with recombinant human IL-4, CD40L, and 30% of human melanoma A375 conditioned medium (CM). IL-4, CD40L, or A375 CM alone had no effect on c-Maf expression in human B cells whereas the combination of IL-4, CD40L and A375 CM significantly upregulated c-Maf expression (figure 6A). Consequently, the combination of IL-4, CD40L and A375 CM significantly upregulated IL-10 production by human B

cells, and inhibition of c-Maf using c-Maf inhibitor Nivalenol (NIV) downregulated IL-10 production by B cells (figure 6B). We further examined human IgG1^+ B cell differentiation, A375 CM treatment significantly downregulated IL-4 plus CD40L induced human IgG1^+ B cell differentiation (online supplemental figure 4A).

Next, we examined B cell profiling and c-Maf expression in the PBMC of HD and patients with melanoma with tumor-negative and tumor-positive sentinel LN (SLN) using CyTOF. FlowSOM analysis identified six major B cell subsets and nine small populations after gating on CD19 and CD20 double-positive B cells. Relatively low c-Maf expression was observed in several subsets, such as populations 1, 8, 12, and 13 (figure 6C). CD27 is one of the most used markers to define human memory B cells.[38] Three CD27^+ B cell subsets (populations 2, 4, and 3) were accumulated in the peripheral blood of SLN-negative patients with melanoma and remarkably reduced in SLN-positive patients. Similarly, SLN-negative patients with melanoma had an increased subset of CD27^-CD38^+ B cells (population 0), representing a transitional B cell phenotype.[39] This subset was decreased in SLN-positive patients compared with that in SLN-negative patients and HD (figure 6D). The changes of CD27^+ B cells and CD27^-CD38^+ B cells were further verified by flow cytometry analysis of PBMC samples (figure 6E). We also calculated the relative proportion of plasmablasts (CD19^+CD20^-CD27^+CD38^+) and showed an increase in plasmablasts in SLN-negative patients with melanoma (figure 6D).

Then, PBMC was cultured with IL-4 and CD40L for 3 days and IL-10 production was examined by intracellular cytokine staining. As shown in figure 6F, IL-10 expression was significantly increased in B cells from patients with melanoma, especially SLN-positive patients. To determine the relationship between c-Maf and IL-10 expression in patients with melanoma, freshly recovered PBMCs from patients with melanoma were restimulated with PMA/Ionomycin/LPS for IL-10 expression. As CD11c is highly expressed in c-Maf positive clusters 1, 8, and 13, we compared IL-10 expression in CD11c^- B cells (no c-Maf expression) and CD11c^+ B cells (c-Maf positive). A significantly higher level of IL-10 was observed in CD11c^+ B cells compared with CD11c^- B cells (figure 6G), suggesting a correlation between c-Maf and IL-10 expression in human B cells. Further, we examined IgG1^+ B cells and no difference was observed in patients with melanoma compared with HD (online supplemental figure 4B).

Lastly, we examined the correlation between c-Maf expression and B cell infiltration by using the publicly available web platform TIMER2.0 (http://timer.cistrome.org). As shown in online supplemental figure 4C, expression of c-Maf is positively correlation with B cell infiltration and CD19 gene expression in melanoma as well as pancreatic adenocarcinoma (PAAD). JAK3 and STAT6 activation is essential in IL-4 signaling pathway.[40] As we observed c-Maf upregulation in the presence of IL-4 and CD40L, we further analyzed the correlation between
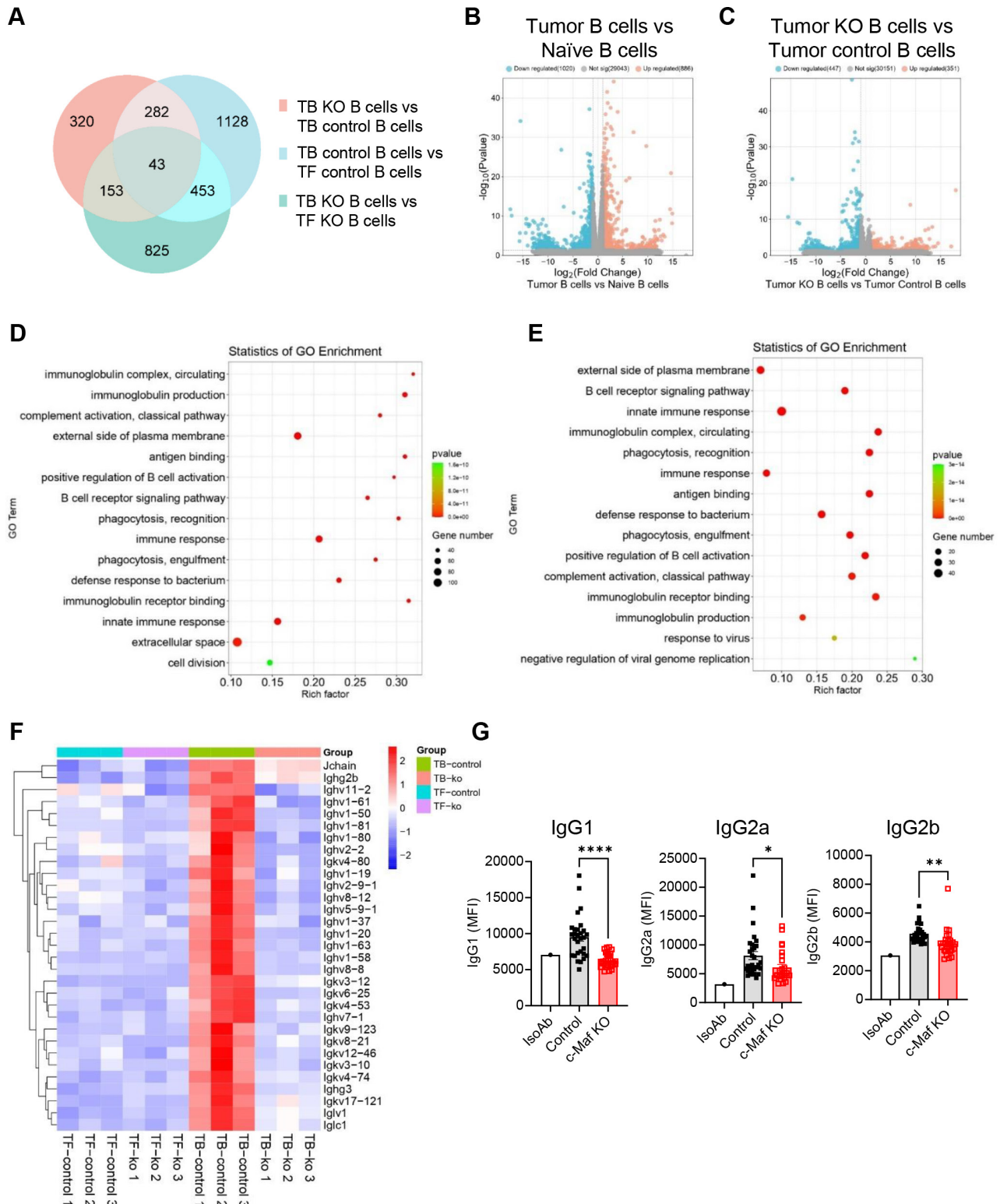
Figure 5 c-Maf regulates immunoglobulin-related genes in B cells and tumor-specific antibody production. (A) Venn diagram showing common and unique genes among the three comparisons. (B) Volcano plot showing fold change (FC) and p value for the comparison of B cells from tumor-bearing versus tumor-free naïve mice (n=3). (C) Volcano plot showing fold change (FC) and p value for the comparison of B cells from tumor-bearing c-Maf KO versus control mice (n=3). (D) GO enrichment analysis of genes defining the 15 most significant terms in B cells from tumor-bearing versus tumor-free naïve mice. (E) GO enrichment analysis of genes defining the 15 most significant terms in B cells from tumor-bearing c-Maf KO versus control mice. (F) Heatmap showing the clustering of immunoglobulin-related genes in four groups based on log-relative abundances. (G) Antitumor specific IgG1, IgG2a, and IgG2b levels in the sera of tumor-bearing mice measured as mean fluorescence intensity (MFI). Each point represents an individual mouse (n=27–29). *p<0.05; **p<0.01; ****p<0.0001. GO, Gene Ontology; Ig, immunoglobulin; KO, knockout; TB, tumor-bearing; TF, tumor-free.
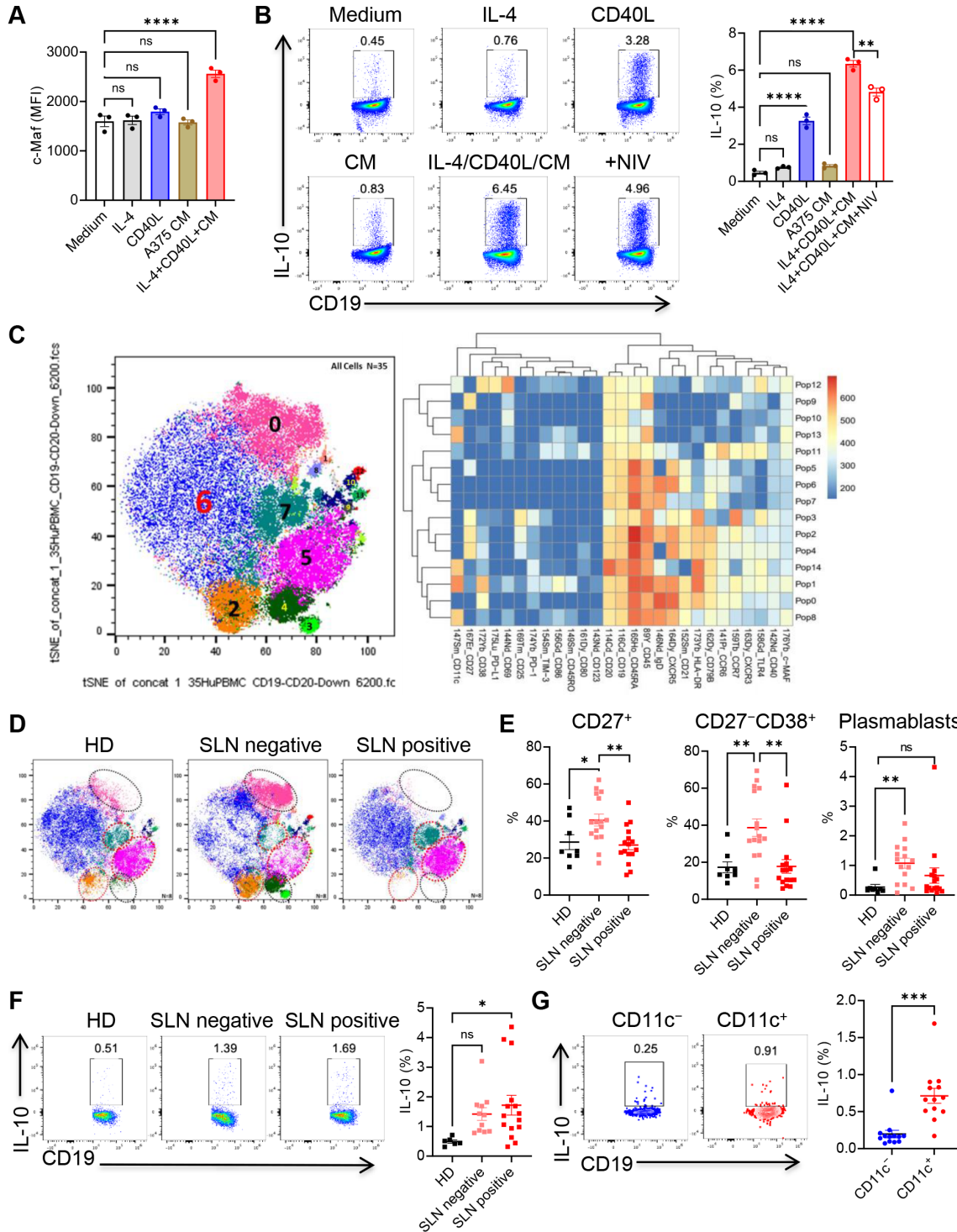
Figure 6 B cell profiling in the peripheral blood of patients with melanoma. (A) Mean fluorescence intensity (MFI) of c-Maf expression in human B cells after 3 days culture. (B) PBMCs were stimulated with IL-4/CD40L and A375 conditioned medium with or without c-Maf inhibitor Nivalenol (0.1 µM). IL-10 production by B cells was determined by intracellular cytokine staining. (C) viSNE analysis of CyTOF immunophenotyping of B cells from healthy donors and patients with melanoma, all samples combined (n=35, left). FlowSOM clustering into 15 B cell subsets showing as a normalized expression heatmap (right). (D) viSNE analysis of CyTOF immunophenotyping in healthy donors and patients with melanoma. (E) Percentages of CD27+ B cells, CD27−CD38+ B cells, and plasmablasts within CD19+ B cells. (F) PBMCs were stimulated with IL-4/CD40L for 3 days followed by PMA/Ionomycin/LPS stimulation for 4 hours. IL-10 production by B cells was determined by intracellular cytokine staining. Each point represents an individual person (n=6–16). (G) Freshly thawed PBMCs from patients with melanoma were stimulated with PMA/Ionomycin/LPS stimulation for 4 hours. IL-10 production by CD11c− and CD11c+ B cells was determined. *p<0.05; **p<0.01; ***p<0.001; ****p<0.0001; ns, not significant. CD40L, CD40 ligand; CM, conditioned medium; CyTOF, mass cytometry; HD, healthy donors; IL-4, interleukin 4; LPS, lipopolysaccharides; NIV, Nivalenol; PBMC, peripheral blood mononuclear cells; PMA, phorbol 12-myristate 13-acetate; SLN, sentinel lymph node.

c-Maf^{+} B cells and IL-4 signature in melanoma and PAAD, the expression of c-Maf was positively correlated with gene expression of JAK3 and STAT6.

Together, these results demonstrate that substantial changes in memory B cells, transitional B cells, and IL-10-producing B cells are correlated with the stage of melanoma and the presence of SLN metastasis.

DISCUSSION

Emerging data have demonstrated that B cells play important roles in tumor progression. However, the role of B cells in antitumor immunity remains controversial. Both protumor and antitumor roles of B cells have been reported in the context of tumor immunology.[8 12 13 19 27] The controversy may be due to the heterogeneity in B cell populations as the balance among the subtypes may impact tumor progression.[19 20 41] Further, tumor type and location are believed to contribute to the complex functions of B cells in antitumor immunity. Therefore, a full understanding of B cells in tumor development is still needed. This study revealed a critical role of c-Maf expression by B cells in promoting tumor growth in two tumor models, PDAC and melanoma.

B cells secrete a very low level of IL-10 at a steady while specific stimulatory signals, such as BCR, CD40, TLR, and cytokine IL-21/IL-6, are involved in the induction of IL-10^{+} B cells. c-Maf is known for the regulation of IL-10 in B cells.[22] Additionally, transcriptional factor STAT3 also modulates IL-10 production.[23] However, the roles of IL-10 in antitumor immunity remain elusive because both protumor and antitumor effects have been reported. For example, IL-10 and PD-1 cooperated to limit tumor-specific CD8^{+} T cells.[38] Blockade of IL-10 potentiated antitumor immune function in human colorectal cancer liver metastases.[39] On the other hand, studies demonstrated that IL-10 can induce antitumor effect by preventing CD8^{+} T cell apoptosis[40] and reprogramming exhausted CD8^{+} T cells.[23 41] Further, IL-10^{+} B cells only represent a relatively small fraction of total B cells. Our data revealed that B16.F10 tumor development increases IL-10 production in B cells from TDLN. However, we observed more circulating follicular B cell accumulation in the pancreas on KPC tumor progression, which led to downregulation of IL-10^{+} B cells. A recent study further reported that loss of B cell specific IL-10 had no effect on B16.F10 melanoma progression.[12] Together, these data suggest that IL-10-independent mechanisms may contribute to the antitumor effect of B cell c-Maf deficiency. In this study, we defined different antitumor mechanisms of B cell c-Maf deficiency in two tumor models. Specifically, c-Maf signaling modulates the proinflammatory phenotype and tumor-specific Ab responses in the KPC tumor-bearing pancreas and TDLN of melanoma, respectively.

Previous studies mainly focused on the production of immunosuppressive cytokines by a small subset of B cells.[14 15 20] We are interested in the evaluation of the overall phenotype of B cells as a whole population in KPC tumor development. Our data demonstrated that B cells display follicular B cell phenotype (CD23^{+}CD21^{low}) on tumor progression, which was associated with an increase of IgD^{+}IgM^{low} B cells. Although the percentage of IL-10^{+} B cells was decreased, isolated total B cells exhibited a decreased antigen-presenting function. A previous study showed that tumor B cells are proinflammatory with upregulation of several proinflammatory cytokines and chemokines which are critical for the recruitment of T cells, macrophages, and dendritic cells.[29] Our RNA-seq analysis and cytokine/chemokine array data further revealed that these proinflammatory cytokines and chemokines are upregulated in c-Maf deficient B cells. A recent study reported that proinflammatory chemokines can boost NK and T cell recruitment leading to immunological tumor control.[34] These data suggest that induction of chemokines through c-Maf inhibition could be a powerful approach to immunologically control PDAC, which is regarded as a "cold" tumor with low T cell and NK cell infiltration in the tumor microenvironment.[42 43] This conclusion is also supported by human studies suggesting that the inflammatory phenotype of B cells is helpful for the antitumor response in the tumor microenvironment.[44 45]

Tumor-specific Abs can either promote tumor growth or exhibit immunostimulatory effects, which may relate to the Ab isotypes.[36 37] Mouse IgG1 (functional equivalent to human IgG4^{+}) has been shown to inhibit antitumor immunity whereas mouse IgG2a/2b (equivalent to human IgG1^{+}) contributes to antitumor immunity.[3 36 46] High IgG/Ig ratio was found to be associated with increased survival probability in melanoma.[47] Our studies revealed the important roles of c-Maf in regulating Ab production. In the mouse B16.F10 melanoma model, the knockdown of c-Maf in B cells resulted in the downregulation of genes related to Ig production and circulating Ig complex. Serum tumor-specific Abs, including IgG1 and IgG2a/2b, were decreased in B cell c-Maf KO tumor-bearing mice. In human B cells, tumor-CM drove down-regulation of human IgG1^{+} B cell differentiation. However, we observed no changes in IgG1^{+} B cell differentiation from PBMC between HD and patients with melanoma. Future studies will investigate how tumor-specific Abs impact tumor progression by studying macrophages in the tumor microenvironment to reveal possible interaction between B cells and macrophages.

Our findings highlight the protumor functions of c-Maf^{+} B cells. Hence, approaches to inhibit c-Maf signaling can be translated into patients with pancreatic cancer and melanoma. Understanding of B cells in antitumor immunity and association with the response to ICB therapies remains insufficient with inconsistent data from studies.[33 48] Given the phenotypic and functional heterogeneity of B cells, further investigation of targeting immunosuppressive B cell subset will lead to the improvement of ICB treatment. A limitation of this study is using the B16.F10 melanoma model which has

very few B cells in the tumor microenvironment. We focus on B cells in TLDN because of their significant expansion and requirement for lymphangiogenesis and melanoma metastasis.[49 50]

MATERIALS AND METHODS
Mice and tumor models
Conditional B cell c-Maf KO mice were generated by intercrossing c-Maf$^{f/f}$ mice[18] with CD19^{Cre} mice (Jackson Laboratory, strain #: 006785). IL-10^{gfp} reporter mice (Vert-X, stain #: 014530) and OT-II transgenic mice (strain #: 004194) were purchased from Jackson Laboratory. Both male and female mice, 6–10 weeks old, were used in studies. PDAC tumor model was established as described in our recent studies.[51 52] 1×10^5 KPC-GFP cells were mixed with Matrigel (Corning) at a 1:1 ratio, and a 50 µl mixture was orthotopically implanted into the tail of the pancreas of 8–10 weeks old B cell c-Maf KO (CD19^{Cre}-c-Maf$^{f/f}$) and control (CD19^{wt}-c-Maf$^{f/f}$) mice. Pancreas were collected at day 18–21 post tumor cell implantation. Pancreas weight and GFP$^+$ tumor cells within viable CD45$^-$ pancreas cells were used to determine the tumor burden. For the melanoma mouse model, 5×10^5 B16.F10 cells in 100 µl phosphate-buffered saline (PBS) were subcutaneously injected into the flank of B cell c-Maf KO and control mice. Tumors were measured two times a week with a caliper. The tumor volumes were calculated using the formula V = (width×width×length)/2. All animal experiments were approved by the Institutional Animal Care and Use Committee of the University of Louisville (#22115).

Preparation of single-cell suspension and flow cytometry
Pancreas were cut into smaller pieces and digested with a digestion buffer comprised of 300 U/mL collagenase I and 80 U/mL DNase (Sigma) in complete RPMI1640 medium for 30 min at 37°C. After incubation, the digestion was immediately stopped by the addition of 5 mL cold complete medium. The suspension was then filtered through a 40 µm cell strainer into petri dishes and extra tissue chunks were further mashed with syringe columns. The red blood cells were lysed by adding ACK lysis buffer for about 1 min and washed two times with a complete medium. For flow cytometry, the cells were blocked in the presence of anti-CD16/CD32 at 4°C for 10 min and stained on ice with the appropriate Abs and isotype controls in PBS containing 1% fetal bovine serum. The fluorochrome-labeled Abs against mouse CD45, CD19, CD21, CD23, CD5, CD43, IgM, IgD, CD9 and their corresponding isotype controls were purchased from BioLegend. Fixable Viability Dye eFluor 780 was from Thermo Fisher Scientific. The samples were acquired using Cytek Aurora cytometry and analyzed using FlowJo software.

INTRACELLULAR STAINING FOR CYTOKINE AND C-MAF EXPRESSION
Cells were stimulated with PMA plus Ionomycin in the presence of protein transport blocker Brefeldin A for 4–6 hours. After staining with surface markers, the cells were then washed, fixed, and permeabilized following BioLegend's protocol. Cells were resuspended in the permeabilization buffer and stained with Abs against mouse IFN-γ and TNF-α, or the respective isotype control overnight at 4°C. For IL-10 production, cells were stimulated with PMA, Ionomycin, and LPS (5 µg/mL) in the presence of Brefeldin A for 4–6 hours followed by intracellular staining using anti-IL-10 Ab. For c-Maf expression measurement, cells were stained with surface markers followed by fixation and permeabilization using eBioscience Foxp3/Transcription Factor Staining Buffer Set. Cells were then stained with anti-human/mouse c-Maf (clone sym0F1, Invitrogen) overnight at 4°C. CD9$^+$CD19$^+$ B cells were further sorted from control and c-Maf KO mice, and c-Maf expression was evaluated by using Western blotting. Abs used in flow cytometry and Western blotting were listed in online supplemental table 1.

B cell stimulation, proliferation, antigen-presenting function, and immunosuppression
Viable CD45$^+$CD19$^+$ B cells were isolated from tumor-free and KPC tumor-bearing pancreas or TDLN by using FACSAria III cell sorter. After carboxyfluorescein succinimidyl ester (CFSE) labeling, cells were stimulated with LPS (1 µg/mL) for 72 hours. B cell proliferation was determined by measuring CFSE division using flow cytometry after staining with anti-mouse CD19 Ab. For the B cell antigen presentation assay, purified B cells were co-cultured with fluorescence activated cell sorting (FACS)-isolated CD3$^+$CD4$^+$ T cells from OT-II transgenic mice in the presence of OVA (200 µg/mL) for 4 days. T cell proliferation was evaluated by measuring CFSE division using flow cytometry. For cytokine and chemokine production, sorted viable CD19$^+$ B cells were stimulated with PMA/Ionomycin/LPS (5 µg/mL) for 24 hours. Expression of cytokine/chemokine in the culture supernatants was measured by using a mouse cytokine array kit (R&D Systems). In some experiments, splenocytes from IL-10^{gfp} reporter mice were cultured with CD40L and BAFF-expressing feeder cells (CD40LB) in the presence of IL-4 (10 ng/mL) for 4 days followed by additional 3 days culture in the presence of IL-21 (20 ng/mL).[53] IL-10$^+$ and IL-10$^-$ B cells were sorted and co-cultured with anti-CD3 mAb-activated CD4$^+$ and CD8$^+$ T cells for 3 days. The IFN-γ production by T cells was evaluated by intracellular cytokine staining and flow cytometry.

Antitumor Ab measurement
Mouse sera were isolated from B16.F10 tumor-bearing mice (day 14–16 after tumor cell inoculation) and incubated with B16.F10 tumor cells at 1:1 dilution at 4°C for 30 min. After two times washing with PBS, cells were stained with fluorescein-conjugated anti-mouse IgG1, IgG2a, IgG2b Abs. The antitumor Abs were determined by measuring mean fluorescence intensity using Flow cytometry.

RNA sequencing and analysis

B cells (CD45$^+$CD19$^+$) were sorted from the pancreas of KPC tumor-bearing mice and TDLN of B16.F10 tumor-bearing mice by using BD FACSAria III. Fixable viability dye was used to exclude dead cells. A post-sort analysis was performed to determine the purity of B cells with approximately 90–95% purity. RNA was extracted using a QIAGEN RNeasy Kit (QIAGEN). The quantity of the purified RNA samples was measured by the RNA High Sensitivity Kit in the Qubit Fluorometric Quantification system (Thermo Fisher Scientific). Library preparation, sequencing, and analysis were performed by LC Sciences (https://lcsciences.com). RNA-seq data (FASTQ files) have been deposited at Sequence Read Archive with reference PRJNA1147765.

HUMAN B CELL DIFFERENTIATION

The PBMCs were isolated from the blood of HD using Ficoll-Hypaque centrifugation. Cells were cultured in complete RPMI1640 medium and stimulated with recombinant human CD40 ligand (CD40L, 500 ng/mL, BioLegend), IL-4 (20 ng/mL), and 30% CM of human melanoma cell line A375. After 3 days of culture, cells were harvested for c-Maf expression measurement using intracellular staining. For IL-10 production, cells were restimulated with PMA/Ionomycin/LPS for 4–6 hours in the presence of Brefeldin A. IL-10 production in B cells was measured by using intracellular cytokine staining. In some experiments, cells were cultured in the presence of c-Maf inhibitor NIV (100 nM; Cayman Chemical).

PBMC collection from patients with melanoma

8–10 mL of peripheral blood was collected from treatment-naïve patients with melanoma including both tumor-negative and tumor-positive SLN at the Department of Surgery, University of Louisville. SLN-positive or SLN-negative was defined as evidence, or no evidence of metastatic tumor cells identified by standard H&E staining and immunohistochemistry. All samples were anonymously coded in accordance with UofL institutional review board (IRB) guidelines, and written informed consent was obtained. The PBMCs were isolated from blood and frozen at −140°C until subsequent analysis.

CyTOF mass cytometry data acquisition and data analysis

Cells from TDLN of B16.F10 tumor-bearing mice were stimulated with PMA, Ionomycin, and LPS in the presence of Brefeldin A for 4–6 hours at 37°C. Cell permeabilization and staining were performed according to the protocol from Fluidigm. Prior to the acquisition, cells were suspended in a 1:9 solution of cell acquisition solution: EQ 4 element calibration beads (Fluidigm) at an appropriate concentration at no more than 600 events per second. Data acquisition was performed on the CyTOF Helios system (Fluidigm). Flow cytometry Standard standard (FCS) files were normalized with the Helios instrument work platform (FCS Processing)

based on the calibration bead signal used to correct any variation in detector sensitivity. CyTOF data analysis was performed with FlowJo software. Total CD45$^+$ cells were gated after removing beads, doublets, and dead cells. The t-distributed stochastic neighbor embedding (tSNE) and FlowSOM clustering analysis for CyTOF data were performed using the FlowJo Plugins platform. tSNE analysis was performed on all samples combined. Different immune populations were defined by the expression of specific surface and intracellular markers.

For human B cell profiling, PBMCs from HD (n=8) and patients with melanoma with tumor-negative SLN (n=16) and tumor-positive SLN (n=16) were used for CyTOF analysis. Cell permeabilization and staining were performed according to the protocol from Fluidigm. Total B cells were gated on CD19 and CD20 double positive cells after removing beads, doublets, and dead cells followed by tSNE and FlowSOM clustering analysis. Abs used for CyTOF were listed in online supplemental tables 2 and 3. The CyTOF (FCS files) have been uploaded to Figshare (https://figshare.com/authors/Chuanlin_DING/19321330).

STATISTICAL ANALYSIS

Data were analyzed using GraphPad Prism software (GraphPad Software). An unpaired Student t-test and one-way or two-way analysis of variance were used to calculate significance, as appropriate. All graph bars are expressed as mean±SEM. Significance was assumed to be reached at $p < 0.05$. The p values were presented as follows: *$p < 0.05$, **$p < 0.01$, ***$p < 0.001$, and ****$p < 0.0001$.

Patient consent for publication All blood samples were anonymously coded in accordance with UofL IRB guidelines, and written informed consent was obtained. This study was approved by the institutional review boards (IRB) of University of Louisville (#08.0491).

Ethics approval This study involves human participants and was approved by the institutional review boards (IRB) of University of Louisville (#08.0491). Participants gave informed consent to participate in the study before taking part.

Provenance and peer review Not commissioned; externally peer reviewed.

Data availability statement Data are available in a public, open access repository. The RNA-seq data (fastq files) have been deposited at Sequence Read Archive: Roles of B cell c-Maf signaling in regulating anti-tumor immunit (PRJNA1147765). The CyTOF data (fcs files) have been uploaded to Figshare (https://figshare.com/authors/Chuanlin_DING/19321330). All other data are available upon reasonable request.

ORCID iDs
Jun Yan http://orcid.org/0000-0003-2922-422X
Chuanlin Ding http://orcid.org/0000-0001-9588-6403

REFERENCES

1. Gunderson AJ, Kaneda MM, Tsujikawa T, *et al*. Bruton Tyrosine Kinase-Dependent Immune Cell Cross-talk Drives Pancreas Cancer. *Cancer Discov* 2016;6:270–85.
2. Lee KE, Spata M, Bayne LJ, *et al*. Hif1a Deletion Reveals Pro-Neoplastic Function of B Cells in Pancreatic Neoplasia. *Cancer Discov* 2016;6:256–69.
3. Gu Y, Liu Y, Fu L, *et al*. Tumor-educated B cells selectively promote breast cancer lymph node metastasis by HSPA4-targeting IgG. *Nat Med* 2019;25:312–22.
4. Ganti SN, Albershardt TC, Iritani BM, *et al*. Regulatory B cells preferentially accumulate in tumor-draining lymph nodes and promote tumor growth. *Sci Rep* 2015;5:12255.
5. du Bois H, Heim TA, Lund AW. Tumor-draining lymph nodes: At the crossroads of metastasis and immunity. *Sci Immunol* 2021;6:eabg3551.
6. Reticker-Flynn NE, Zhang W, Belk JA, *et al*. Lymph node colonization induces tumor-immune tolerance to promote distant metastasis. *Cell* 2022;185:1924–42.
7. Singh S, Roszik J, Saini N, *et al*. B Cells Are Required to Generate Optimal Anti-Melanoma Immunity in Response to Checkpoint Blockade. *Front Immunol* 2022;13:794684.
8. Downs-Canner SM, Meier J, Vincent BG, *et al*. B Cell Function in the Tumor Microenvironment. *Annu Rev Immunol* 2022;40:169–93.
9. Qin Y, Peng F, Ai L, *et al*. Tumor-infiltrating B cells as a favorable prognostic biomarker in breast cancer: a systematic review and meta-analysis. *Cancer Cell Int* 2021;21:310.
10. Fridman WH, Meylan M, Petitprez F, *et al*. B cells and tertiary lymphoid structures as determinants of tumour immune contexture and clinical outcome. *Nat Rev Clin Oncol* 2022;19:441–57.
11. Romero D. B cells and TLSs facilitate a response to ICI. *Nat Rev Clin Oncol* 2020;17:195.
12. Bod L, Kye Y-C, Shi J, *et al*. B-cell-specific checkpoint molecules that regulate anti-tumour immunity. *Nature New Biol* 2023;619:348–56.
13. Wang Z, Lu Z, Lin S, *et al*. Leucine-tRNA-synthase-2-expressing B cells contribute to colorectal cancer immunoevasion. *Immunity* 2022;55:1748.
14. Li S, Mirlekar B, Johnson BM, *et al*. STING-induced regulatory B cells compromise NK function in cancer immunity. *Nature New Biol* 2022;610:373–80.
15. Pylayeva-Gupta Y, Das S, Handler JS, *et al*. IL35-Producing B Cells Promote the Development of Pancreatic Neoplasia. *Cancer Discov* 2016;6:247–55.
16. Imbratta C, Hussein H, Andris F, *et al*. c-MAF, a Swiss Army Knife for Tolerance in Lymphocytes. *Front Immunol* 2020;11:206.
17. Liu M, Tong Z, Ding C, *et al*. Transcription factor c-Maf is a checkpoint that programs macrophages in lung cancer. *J Clin Invest* 2020;130:131335:2081–96:.
18. Chen X, Cai Y, Hu X, *et al*. Differential metabolic requirement governed by transcription factor c-Maf dictates innate γδT17 effector functionality in mice and humans. *Sci Adv* 2022;8:eabm9120.
19. Conejo-Garcia JR, Biswas S, Chaurio R, *et al*. Neglected no more: B cell-mediated anti-tumor immunity. *Semin Immunol* 2023;65:101707.
20. Mirlekar B, Wang Y, Li S, *et al*. Balance between immunoregulatory B cells and plasma cells drives pancreatic tumor immunity. *Cell Rep Med* 2022;3:100744.
21. Radomir L, Kramer MP, Perpinial M, *et al*. The survival and function of IL-10-producing regulatory B cells are negatively controlled by SLAMF5. *Nat Commun* 2021;12:1893.
22. Liu M, Zhao X, Ma Y, *et al*. Transcription factor c-Maf is essential for IL-10 gene expression in B cells. *Scand J Immunol* 2018;88:e12701.
23. Michée-Cospolite M, Boudigou M, Grasseau A, *et al*. Molecular Mechanisms Driving IL-10- Producing B Cells Functions: STAT3 and c-MAF as Underestimated Central Key Regulators? *Front Immunol* 2022;13:818814.
24. Hillion S, Miranda A, Le Dantec C, *et al*. Maf expression in B cells restricts reactive plasmablast and germinal center B cell expansion. *Nat Commun* 2024;15:7982.
25. Sun J, Wang J, Pefanis E, *et al*. Transcriptomics Identify CD9 as a Marker of Murine IL-10-Competent Regulatory B Cells. *Cell Rep* 2015;13:1110–7.
26. Fridman WH, Petitprez F, Meylan M, *et al*. B cells and cancer: To B or not to B? *J Exp Med* 2021;218:e20200851.
27. Shalapour S, Karin M. The neglected brothers come of age: B cells and cancer. *Semin Immunol* 2021;52:101479.
28. Popi AF, Lopes JD, Mariano M. Interleukin-10 secreted by B-1 cells modulates the phagocytic activity of murine macrophages in vitro. *Immunology* 2004;113:348–54.
29. Spear S, Candido JB, McDermott JR, *et al*. Discrepancies in the Tumor Microenvironment of Spontaneous and Orthotopic Murine Models of Pancreatic Cancer Uncover a New Immunostimulatory Phenotype for B Cells. *Front Immunol* 2019;10:542.
30. Guo L, Li N, Yang Z, *et al*. Role of CXCL5 in Regulating Chemotaxis of Innate and Adaptive Leukocytes in Infected Lungs Upon Pulmonary Influenza Infection. *Front Immunol* 2021;12:785457.
31. Ren G, Al-Jezani N, Railton P, *et al*. CCL22 induces pro-inflammatory changes in fibroblast-like synoviocytes. *i Sci* 2021;24:101943.
32. Pandey V, Fleming-Martinez A, Bastea L, *et al*. CXCL10/CXCR3 signaling contributes to an inflammatory microenvironment and its blockade enhances progression of murine pancreatic precancerous lesions. *Elife* 2021;10:e60646.
33. Griss J, Bauer W, Wagner C, *et al*. B cells sustain inflammation and predict response to immune checkpoint blockade in human melanoma. *Nat Commun* 2019;10:4186.
34. Chibaya L, Murphy KC, DeMarco KD, *et al*. EZH2 inhibition remodels the inflammatory senescence-associated secretory phenotype to potentiate pancreatic cancer immune surveillance. *Nat Cancer* 2023;4:872–92.
35. Yoshizaki A, Miyagaki T, DiLillo DJ, *et al*. Regulatory B cells control T-cell autoimmunity through IL-21-dependent cognate interactions. *Nature New Biol* 2012;491:264–8.
36. Higgins BW, McHeyzer-Williams LJ, McHeyzer-Williams MG. Programming Isotype-Specific Plasma Cell Function. *Trends Immunol* 2019;40:345–57.
37. Sharonov GV, Serebrovskaya EO, Yuzhakova DV, *et al*. B cells, plasma cells and antibody repertoires in the tumour microenvironment. *Nat Rev Immunol* 2020;20:294–307.
38. Grimsholm O. CD27 on human memory B cells-more than just a surface marker. *Clin Exp Immunol* 2023;213:164–72.
39. Sanz I, Wei C, Jenks SA, *et al*. Challenges and Opportunities for Consistent Classification of Human B Cell and Plasma Cell Populations. *Front Immunol* 2019;10:2458.
40. Davey EJ, Greicius G, Thyberg J, *et al*. STAT6 is required for the regulation of IL-4-induced cytoskeletal events in B cells. *Int Immunol* 2000;12:995–1003.
41. Tsou P, Katayama H, Ostrin EJ, *et al*. The Emerging Role of B Cells in Tumor Immunity. *Cancer Res* 2016;76:5597–601.
42. Ullman NA, Burchard PR, Dunne RF, *et al*. Immunologic Strategies in Pancreatic Cancer: Making Cold Tumors Hot. *J Clin Oncol* 2022;40:2789–805.
43. Joseph AM, Al Aiyan A, Al-Ramadi B, *et al*. Innate and adaptive immune-directed tumour microenvironment in pancreatic ductal adenocarcinoma. *Front Immunol* 2024;15:1323198.
44. Castino GF, Cortese N, Capretti G, *et al*. Spatial distribution of B cells predicts prognosis in human pancreatic adenocarcinoma. *Oncoimmunology* 2016;5:e1085147.
45. Tewari N, Zaitoun AM, Arora A, *et al*. The presence of tumour-associated lymphocytes confers a good prognosis in pancreatic ductal adenocarcinoma: an immunohistochemical study of tissue microarrays. *BMC Cancer* 2013;13:436.
46. Karagiannis P, Gilbert AE, Josephs DH, *et al*. IgG4 subclass antibodies impair antitumor immunity in melanoma. *J Clin Invest* 2013;123:1457–74.
47. Crescioli S, Correa I, Ng J, *et al*. B cell profiles, antibody repertoire and reactivity reveal dysregulated responses with autoimmune features in melanoma. *Nat Commun* 2023;14:3378.

48 de Jonge K, Tillé L, Lourenco J, *et al*. Inflammatory B cells correlate with failure to checkpoint blockade in melanoma patients. *Oncoimmunology* 2021;10:1873585.

49 Harrell MI, Iritani BM, Ruddell A. Tumor-induced sentinel lymph node lymphangiogenesis and increased lymph flow precede melanoma metastasis. *Am J Pathol* 2007;170:774–86.

50 Ruddell A, Harrell MI, Furuya M, *et al*. B lymphocytes promote lymphogenous metastasis of lymphoma and melanoma. *Neoplasia* 2011;13:748–57.

51 Geller AE, Shrestha R, Woeste MR, *et al*. The induction of peripheral trained immunity in the pancreas incites anti-tumor activity to control pancreatic cancer progression. *Nat Commun* 2022;13:759.

52 Woeste MR, Shrestha R, Geller AE, *et al*. Irreversible electroporation augments β-glucan induced trained innate immunity for the treatment of pancreatic ductal adenocarcinoma. *J Immunother Cancer* 2023;11:e006221.

53 Dascani P, Ding C, Kong X, *et al*. Transcription Factor STAT3 Serves as a Negative Regulator Controlling IgE Class Switching in Mice. *Immunohorizons* 2018;2:349–62.